Proceedings of the 20th International Conference on Soil Mechanics and Geotechnical Engineering– Rahman and Jaksa (Eds)

An efficient scheme for the calculation of unsaturated flow in geomaterials with coarse textures

Un schéma efficace pour le calcul de l'écoulement non saturé dans les géomatériaux à textures grossières

Denis Maier, Héctor Montenegro & Bernhard Odenwald
Department of Geotechnical Engineering, BAW Karlsruhe, Germany

Abstract

Based on an extensive series of variably flow computations of a representative engineering problem comprising infiltration into rather dry soils of wide range of soil texture the performance of a novel approach was assessed. Casulli's scheme eliminates numerical problems intrinsically associated with the non-linear behavior of water retention characteristics via a remarkably simple decomposition into two monotonically increasing functions. Casulli's scheme proved superior to established methods in respect to stability as it converged within rather large time steps. The identified robustness of the novel scheme comprises a certain loss in efficiency in terms of the execution rate. From the perspective of engineering practice, in which infiltration scenarios in rather coarse textured soils and dry initial conditions are quite frequent the compromise between robustness and execution duration is more than acceptable. In the context of coupled flow-deformation analyses the advantages of constant and rather large time steps offered by Casulli's scheme will certainly prove as the method of choice.

RÉSUMÉ

Sur la base d'une vaste série de calculs à débit variable d'un problème d'ingénierie représentatif comprenant l'infiltration dans des sols plutôt secs d'une large gamme de textures de sol, les performances d'une nouvelle approche ont été évaluées. Le schéma de Casulli élimine les problèmes numériques intrinsèquement associés au comportement non linéaire des caractéristiques de rétention d'eau via une décomposition remarquablement simple en deux fonctions monotones croissantes. Le schéma de Casullis s'est avéré supérieur aux méthodes établies en ce qui concerne la stabilité car il a convergé dans des pas de temps assez grands. La robustesse identifiée du nouveau schéma comprend une certaine perte d'efficacité en termes de taux d'exécution. Du point de vue de la pratique de l'ingénierie, dans laquelle les scénarios d'infiltration dans des sols à texture assez grossière et des conditions initiales sèches sont assez fréquents, le compromis entre robustesse et durée d'exécution est plus qu'acceptable. Dans le contexte des analyses couplées flux-déformation, les avantages des pas de temps constants et assez grands offerts par le schéma de Casulli s'avéreront certainement comme la méthode de choix.

KEYWORDS: 3D variably saturated flow, Finite volume method, coarse textured soils, infiltration into dry soils

1 INTRODUCTION

Fluid–structure interaction problems appear in many engineering applications, e.g., in the design of excavations, earthen dams and other geotechnical structures. In many problems it is necessary to predict hydromechanical behavior under consideration of variably saturated flow transitions from full to partial saturation. This work focusses on the assessment of two different approaches for the computation of variably saturated flow in terms of robustness and effectiveness considering the wide range of texture in soils and geomaterials as well as initial moisture conditions typically encountered in engineering practice.

1.1 *Non-linearity in variably saturated flow*

Variably saturated flow problems require iterative schemes due to the nonlinear character of the equation system to be solved. Although Newton's method exhibits fast (typically quadratic) convergence, it's sensitivity to initial solution estimates ensues a serious drawback. While the modified Picard algorithm proposed by Celia et al. (1990) is more robust it may exhibit rather slow convergence rates. Unfortunately, both methods tend to fail for problems common in geotechnical engineering, considering infiltration into rather dry soils. The considerably non-linear nature of hydraulic soil properties is generally considered as responsible for such problems.

Casulli and Zanolli (2010) presented a scheme for which they revealed an enhanced monotonicity and superior robustness with an augmented convergence rate for any time step size. These qualities make this scheme very appealing particularly in the context of coupled models (flow-deformation, flow transport etc.). While the established Celia algorithm may yield equivalent results with a variable time stepping technique, in the context of coupled problems time step adaptation to the convergence behavior may involve superfluous solutions of the coupled processes involved.

The remainder of this presentation is organized as follows. In section 2 the governing equations for variably saturated flow are presented and the focal aspects of Casulli's scheme introduced. Next a representative problem from engineering practice which is known to produce severe numerical problems even under rather habitual circumstances is illustrated in section 3. The two approaches are compared in terms of efficiency and robustness in section 4. Finally hints and remarks on the implementation are summarized in section 5.

2 GOVERNING EQUATIONS

In the framework of variably saturated flow, fluid mass conservation is expressed by the so-called mixed form of Richards' equation (1), where

$$\mathrm{p} = \frac{1}{\gamma_w}(p_w - p_a) \tag{1}$$

is the pressure head with γ_w is the specific weight of water and p_a, p_w are the pore-air pressure and pore-water pressure, respectively.

$$\partial_t\, \theta\,(\mathrm{p}) = \nabla[K(x, \theta\,(\mathrm{p}))[\nabla(\mathrm{p} + Z)]] \tag{1}$$

θ(p) represents the water content, K denotes the hydraulic conductivity, which may vary with location x and water content. Z is the height against the gravitational direction in respect to an arbitrary reference level. The gas within the pore-space is consider to be under atmospheric pressure ($\mathrm{p}_a \equiv 0$) at all time. The water content θ(p) exhibits a nonlinear relation to pressure head (soil water characteristic curve or water retention curve). Since with decreasing water content, less pores are water filled and can participate in the conduction of water, the hydraulic conductivity is a (nonlinear) function of water content and therefore in pressure head as well. These functional relations are typically prescribed by constitutive models, of which the van Genuchten-Mualem Model (2) is the most prominent.

$$\theta\,(\mathrm{p}) = \begin{cases} \theta_r + \dfrac{\theta_s - \theta_r}{[1 + |\alpha \mathrm{p}|^n]^m} & \text{for } \mathrm{p} \le 0 \\ \theta_s & \text{for } \mathrm{p} > 0 \end{cases} \tag{2a}$$

$$K\,(\mathrm{x}, \theta) = K\,(\mathrm{x}) \left(\frac{\theta - \theta_r}{\theta_s - \theta_r}\right)^{\frac{1}{2}} \left(1 - \left[1 - \left(\frac{\theta - \theta_r}{\theta_s - \theta_r}\right)^{\frac{1}{m}}\right]^m\right)^2 \tag{2b}$$

Direct measurements are to be conducted for estimation of the hydraulic model parameters. θ_r and θ_s denote the residual ($\mathrm{p} \to -\infty$) and the saturated ($\mathrm{p} \to 0$) water content, respectively. The remaining parameters, namely α, n and m are parameters determining the exact shape of the relations of the saturation and the hydraulic conductivity with pressure head.

In this contribution, cell centered finite volumes is used to discretize (1) in space and the Euler backwards scheme for time discretization. Nonetheless, the following derivation hold independently of the specific discretization preferred. The discretized form of (1) is a system of nonlinear equations:

$$\boldsymbol{\theta}\,(\mathrm{p}^t) + \boldsymbol{\Phi}(\mathrm{p}^t)\,\mathrm{p}^t = \mathbf{R}(\,\mathrm{p}^{t-1}) \tag{2}$$

The Matrix $\boldsymbol{\theta}\,(\mathrm{p}^t)$ contains the water contents of the discretization elements (Mass Matrix), $\boldsymbol{\Phi}(\mathrm{p}^t)$ is the (Darcian) Flux Matrix owing to pressure gradients and the right-hand side (**R**) contains the discretized fluxes due to gravitation and water content values $\theta\,(\mathrm{p}^{t-1})$ from the previous timestep.

The Newton method, as stated earlier, is the quasi-standard method for the linearization of strongly nonlinear systems. The nonlinearity in the case of system (2) resides in the terms in the matrices $\boldsymbol{\theta}\,(\mathrm{p}^t)$ and $\boldsymbol{\Phi}(\mathrm{p}^t)$. However, since Newton's Method demands an initial approximate quite close to the desired solution, the approach becomes impractical for general usage.

Many variations and adaptations of Newton's methods (e.g. Celia et al. 1990, List & Radu 2016) have been proposed and, to a degree, been employed with great success. However, high nonlinearities in the constitutive relations for coarse, rather dry materials still seem to be a major problem for most schemes. The general framework for the successful linearization of system (2) stems from Celia et al. (1990) in which the hydraulic conductivity term is linearized by a Picard fixed-point iteration while the water content is linearized by a linear Taylor-Series expansion similar to Newton's method.

With $\mathrm{p}^{t,0} = \mathrm{p}^{t-1}$ as initial guess, this leads to the linearized system of equation with t and n denoting the time and iteration index respectively:

$$\boldsymbol{\theta}\,(\mathrm{p}^{t,n-1}) + \boldsymbol{C}(\mathrm{p}^{t,n-1})(\mathrm{p}^{t,n} - \mathrm{p}^{t,n-1}) + \boldsymbol{\Phi}(\mathrm{p}^{t,n-1})\,\psi^{t,n} = \mathbf{R}(\,\mathrm{p}^{t-1}) \tag{3}$$

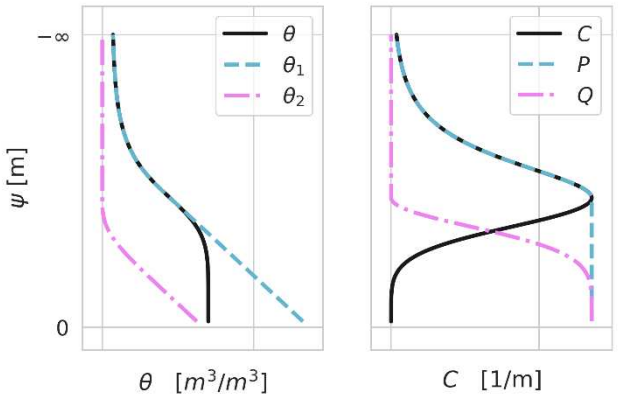

Figure 1. Decomposition of the water content θ(p) (left) and water capacity C(p) (right) in two nondecreasing functions of pressure head p.

Most linearization schemes differ in the approximation of the Jacobian $\boldsymbol{C}(\mathrm{p}) = \boldsymbol{\partial}_{\mathrm{p}}\boldsymbol{\theta}(\mathrm{p})$. It is called soil water capacity and represents the water storage and release capabilities of a soil.
To remedy convergence of the linearization scheme (3) even for very dry and coarse materials, Casulli and Zanolli (2010) proposed an extension to the treatment of the water capacity term. The peak in the water capacity function $\boldsymbol{C}(\mathrm{p})$ has been identified as cause for convergence problems of algorithm (3) and Jordan decomposition of C(p) into two monotonic increasing functions $\boldsymbol{C}(\mathrm{p}) = \mathrm{P}(\mathrm{p}) - \mathrm{Q}(\mathrm{p})$ was suggested as shown in Figure 1. Consequently, through independent integration (see (4)) of the decomposed water capacity subfunctions, the water retention curve is decomposed as well into two water contents $\boldsymbol{\theta} = \boldsymbol{\theta_1} - \boldsymbol{\theta_2}$ (s. Figure 1).

$$\boldsymbol{\theta_1}\,(\mathrm{p}) = \theta_r + \int_{-\infty}^{\mathrm{p}} \boldsymbol{P}\,(\hat{\mathrm{p}})\, d\hat{\mathrm{p}} \tag{4a}$$

$$\boldsymbol{\theta_2}\,(\mathrm{p}) = \int_{-\infty}^{\mathrm{p}} \boldsymbol{Q}\,(\hat{\mathrm{p}})\, d\hat{\mathrm{p}} \tag{4b}$$

After decomposition of $\boldsymbol{\theta}$ the system of equations becomes

$$\boldsymbol{\theta_1}\,(\mathrm{p}^{t,n}) - \boldsymbol{\theta_2}\,(\mathrm{p}^{t,n}) + \boldsymbol{\Phi}(\mathrm{p}^{t,n-1})\,\mathrm{p}^t = \mathbf{R}(\,\mathrm{p}^{t-1}) \tag{5a}$$

Q being the Jacobian for $\boldsymbol{\theta_2}$, Newton's method applied only to the second term and, for the sake of readability, omitting the time and iteration indices (t, n) (5a) is expressed with the outer Casulli iterates $\{\psi^k\} = \{\psi^{t,n,k}\}$ as:

$$\boldsymbol{\theta_1}\,(\mathrm{p}^k) - \boldsymbol{\theta_2}\,(\mathrm{p}^{k-1}) - \boldsymbol{Q}(\mathrm{p}^{k-1})(\mathrm{p}^k - \mathrm{p}^{k-1}) + \boldsymbol{\Phi}\,\mathrm{p}^k = \mathbf{R} \tag{5b}$$

The initial guess $\mathrm{p}^0 = \mathrm{p}^{n-1}$ is the solution of the previous Picard iteration. Linearizing the first term accordingly yields a nested Newton-type algorithm with inner iterates $\{\mathrm{p}^{k,l}\} = \{\mathrm{p}^{t,n,k,l}\}$:

$$\boldsymbol{\theta_1}\,(\mathrm{p}^{k,l-1}) + \boldsymbol{P}(\mathrm{p}^{k,l-1})(\mathrm{p}^{k,l} - \mathrm{p}^{k,l-1}) - \boldsymbol{\theta_2}\,(\mathrm{p}^{k-1}) - \boldsymbol{Q}(\mathrm{p}^{k-1})(\mathrm{p}^{k,l} - \mathrm{p}^{k-1}) + \boldsymbol{\Phi}\,\mathrm{p}^{k,l} = \mathbf{R} \tag{5c}$$

Again, with the solution of the previous outer iteration $\mathrm{p}^{k,0} = \mathrm{p}^{k-1}$ as the initial guess for (5c). This linearization has the advantage that P and Q are monotonic increasing over the whole range.

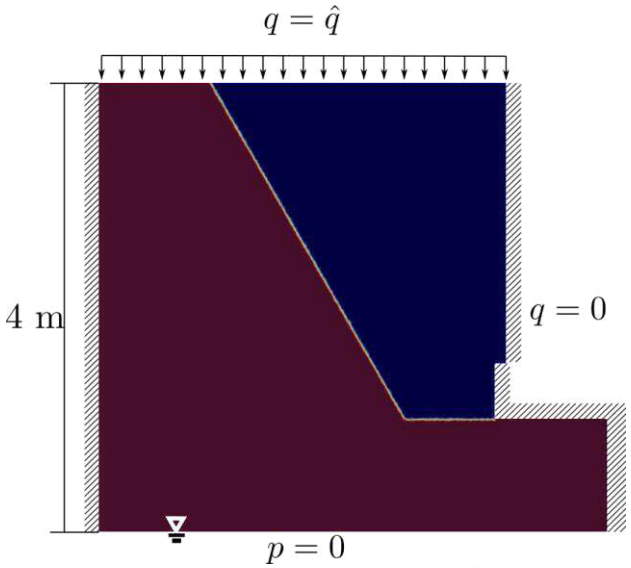

Figure 2. Model problem geometry and boundary conditions.

3 TEST CASE

In order to assess the Casulli scheme (5), a nontrivial 2D test-case from geotechnical engineering practice was set up. The problem concerns with infiltration during 72 hours of precipitation into the backfill along the foundation of a building. The aim of the analysis is to predict the occurrence and duration of saturated zones during or following the extreme rainfall event, and to analyze if waterproofing the structure will be necessary. The geometry and boundary conditions are displayed in Figure 2. The backfill is a coarse-grained sand placed in the excavated gap between the structure and the fine-grained in-situ soil. The unstructured triangular finite volume elements form the calculation mesh with an adequate resolution to represent the hydraulic gradients expected (Figure 2).

3.1 *Hydraulic properties*

A series of calculations were performed with backfill materials of varying hydraulic properties covering the typical span width of textures for this rather coarse-grained material. The corresponding van Genuchten-Mualem parameters are displayed in Table 1. A plot visualizing the parametric curves over pressure head / matric suction for the examined backfill soils is presented in Figure 3 for comparison.

The initial condition represents the antecedent moisture content and represents an important issue in the analysis of infiltration dynamics. Furthermore, due to the non-linearity of the soil hydraulic functions the initial water content of both backfill and in-situ was expected to affect the solver performance. Hence, the initial condition was set according to the steady-state solution of six different ground-water recharge intensities listed in Table 2. This choice considers antecedent moisture conditions I the range from very dry to very wet.

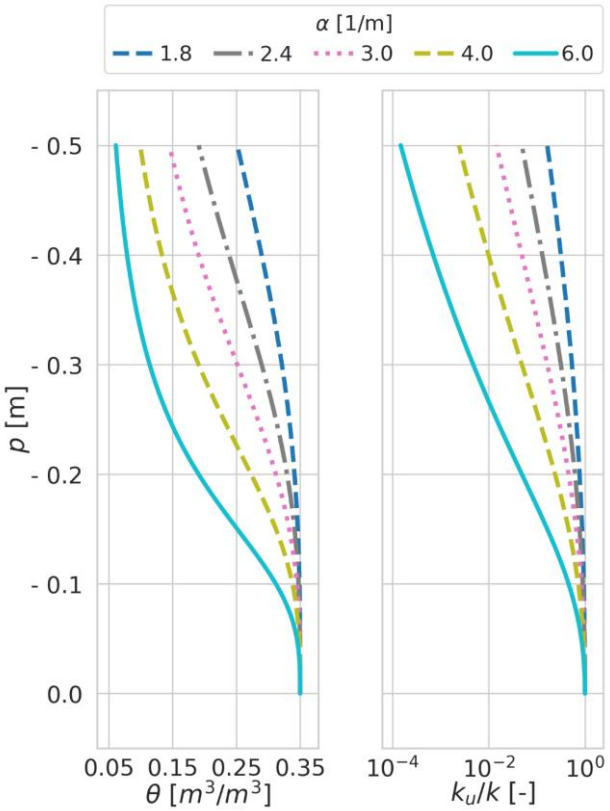

Figure 3. Van Genuchten water content and Mualem relative hydraulic conductivity as functions of pressure head with parameters according to Table 1.

Table 1. Hydraulic properties of the backfill material according the van Genuchten – Mualem parametrization.

	θ_s [-]	θ_r [-]	α [m^{-1}]	n [-]	k[m/s]
In-situ soil	0.40	0.10	0.6	3.1	10^{-7}
backfill 1	0.35	0.03	1.8	3.1	10^{-3}
backfill 2	0.35	0.03	2.4	3.1	10^{-3}
backfill 3	0.35	0.03	3.0	3.1	10^{-3}
backfill 4	0.35	0.03	4.0	3.1	10^{-3}
backfill 5	0.35	0.03	6.0	3.1	10^{-3}

Table 2. Recharge intensities for the steady-state computations of the initial moisture distribution.

case	1	2	3	4	5	6
q_{init} [mm/year]	0	80	160	240	320	400

3.2 *Choice of solver parameters*

Extensive preliminarily testing was carried out to find adequate solver parameters and to allow a fair comparison. For both algorithms, convergence is accepted, if at the end of the Picard iteration step the following conditions are met

$$r^{t,n} = \|\boldsymbol{\theta}(\tilde{\mathrm{p}}^{t,n}) + \boldsymbol{\Phi}(\tilde{\mathrm{p}}^{t,n})\,\tilde{\mathrm{p}}^{t,n} - \mathbf{R}(\mathrm{p}^{t-1})\|_2 \leq \varepsilon \qquad (3)$$

where, r is the L_2 norm of the residuals of equation (2) with the current solution approximation $\tilde{\mathrm{p}}^{t,n}$ and ε is the solution tolerance. We found $\varepsilon = 10^{-5}$ to be acceptable for the studied test case restraining mass balance errors below 5% in each time-step without restricting the convergence. The total of nonlinear iterations was not restricted.

Generally, the linearized system describing variably saturated flow exhibits a superior condition for smaller timesteps. Casulli's Scheme was therefore tested with a rather large timestep size of 1 h and another timestep size of ¼ h to assess the solvers behavior.

4 RESULTS

4.1 *Evaluation of test case results*

Infiltration dynamics are controlled by the soil hydraulic properties, boundary conditions and the initial water content distribution which is prescribed in this study by the antecedent rainfall intensity.

Three different scenarios are displayed in Figure 4 to illustrate the impact of soil properties and initial conditions on the infiltration dynamics. First, in 4A the calculation started assuming a hydrostatic pressure distribution corresponding to no antecedent infiltration rate. In comparison to 4B, with an antecedent precipitation rate of 400 mm/a, the initial conditions are considerably dryer and thus the infiltration front progresses more compressed and at a slower rate in both the in-situ soil and backfill material. The distributions of the specific discharge reveal that in both cases the infiltration front is concentrated at the interface between backfill material and in-situ soil. This results from the lower saturated hydraulic conductivity of the sloped in situ soil. Hence, the moisture content at the interface increases augmenting the unsaturated hydraulic conductivity in this region. In 4C the soil texture of the backfill material is substantially coarser in comparison to 4B as indicated by the contrast of the air entry α parameter of 1.8 to 6.0 [1/m]. The infiltration dynamics particularly in the backfill material display a different characteristic. The infiltration front in the coarser back-fill material is concentrated in the upper part of the interface to the in-situ soil while exhibiting a less pronounced infiltration depth. Interestingly, the infiltration front penetrates the coarser backfill material in a sharper fashion compared to the other two cases, which is best visualized by the pressure head variation with time at point P (see fig.4A) in figure 5.

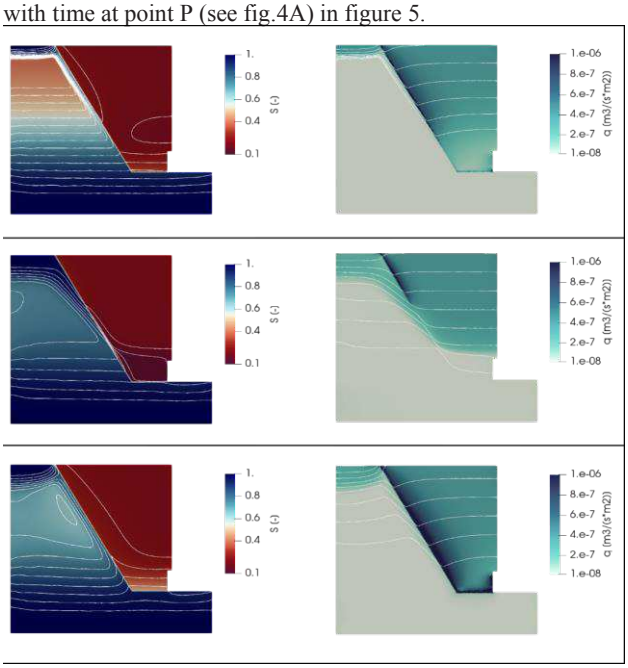

Figure 4. Saturation distribution, isobars (top), potential lines and specific discharge rate q (bottom) for three sets of initial conditions and soil texture at 42 h after the beginning of rainfall. A: q_{init} = 0 mm/a, α = 1.8 1/m; B: q_{init} = 400 mm/a, α = 1.8 1/m; C: q_{init} = 400 mm/a, α = 6 1/m.

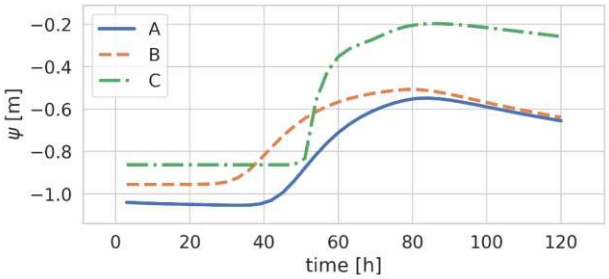

Figure 5. Time variation curve of pressure head ψ at point P (see fig. 4A). A: q init = 0mm/a, α = 1.8 1/m; B: q init = 400mm/a, α = 1.8 1/m; C: q init = 400mm/a, α = 6 1/m

A lower antecedent water content essentially delays the infiltration front. Soil properties corresponding to a coarser soil (increased air entry parameter α) slow down the infiltration front as well due to the rapid drop in unsaturated conductivity at the wetting edge of the front. Consequently, the infiltration front becomes sharper eventually creating sort of a breakthrough zone and a substantially increased peak pressure.

4.2 *Remarks on solver performance*

Unsaturated flow computations in rather coarse soils and at low water contents are rather frequent in engineering practice. In the unsaturated flow analysis these circumstances turn out to be quite demanding due to the non-linearity comprised with large variations in storage and unsaturated conductivity with small changes in moisture. In this study solver performance is evaluated in respect to soil texture (expressed through the air entry parameter α) and antecedent moisture conditions, respectively. Figure 6 shows mean execution times over initial conditions against the air-entry parameter α, representing coarser soil texture with higher α-values. The Celia-Scheme mentioned above was considered used as the reference "standard"-solver, due to its numerous implementations in commercial software. The same convergence criterion (3) is set for both schemes to ensure a fair comparison. For Celia's scheme a time step size of ¼ h had to be applied, since larger timesteps proved as non-convergent in the vast majority of test runs.

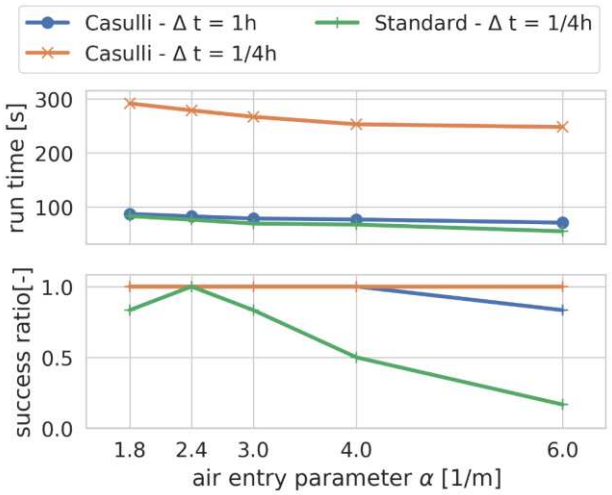

Figure 6. **Top:** Execution (run) times for Casulli's scheme with 1 h and ¼ h timestep and a standard scheme (Celia) against the air entry parameter α. **Bottom:** Success rations for the same solvers in respect to the air entry parameter α.

Casulli's scheme required essentially the same execution time independent of the soil texture for the studied parameter sets. Comparing the 1 h time step scheme to the ¼ h time step in the standard scheme, execution speeds are comparable. Reducing the

timestep with the Casulli scheme, however, is costly as execution times increases considerably. The curves at the bottom of figure 6 display the success ratios of each scheme with respect to soil texture. The success ratio is defined here as the amount of calculations that finished (converged) divided by the total sum of calculations with the same air-entry parameter. The success ratios in figure 5 display the benefits of allowing longer execution times. While comparably slow, the Casulli Scheme with ¼ h time step delivers a convergence to 100% of the test cases. On the other hand, the Casulli Scheme with 1 h timestep fails for just one case and that is the one with the coarsest texture. The decline of the success ratios for the standard scheme reveals that higher α-values tend to be more demanding for that solver. Analogous conclusions can be drawn examining the runs in respect to antecedent moisture, as displayed in figure 7.

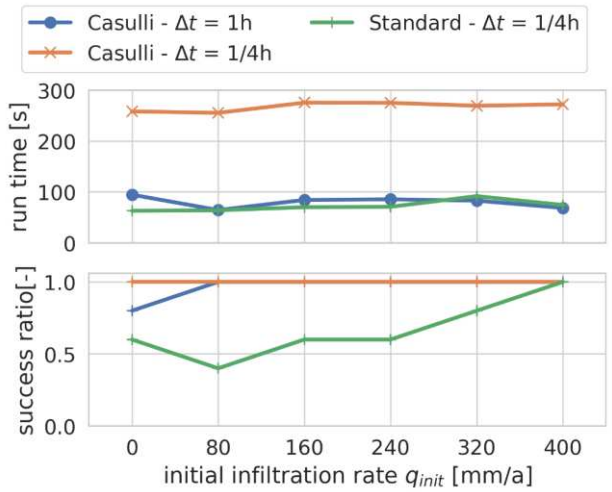

Figure 7. **Top:** Execution (run) times for Casulli's scheme with 1 h and ¼ h timestep and a standard scheme (Celia) against the air entry parameter α. **Bottom:** Success rations for the same solvers in respect to the air entry parameter α.

While the run times curves related to initial infiltration rate (antecedent soil moisture) yield similar results as in the case of texture displayed above, the success ratios show that dryer antecedent moisture conditions tend to be more challenging for both schemes. Again, the slower Casulli's scheme with ¼ h time step yields convergence for all runs and at 1 h timestep converges flawlessly for all but the driest case, both time step variants remaining at a competitive execution speed. On the other hand, the standard solver struggles with dryer conditions shown by the clear decline of the success ratio from wet to dry antecedent moisture conditions.

6 CONCLUSIONS

In a series of model runs of a representative engineering problem comprising varying soil textures and initial soil moisture conditions the performance of a novel approach proposed by Casulli was assessed. Casulli's scheme eliminates notorious numerical problems associated with the non-linear behavior of the soil water characteristic curve through a decomposition into two monotonically increasing functions.

Casulli's method proved to be astonishingly stable, converging for all but the driest initial conditions and coarsest soil textures tested with rather large time steps (1 h). Reducing the timestep size to ¼ h allowed convergence where the 1h scheme failed, however at the cost of computational time.

Providing such benefits particularly in cases considering rather dry initial conditions and coarse textured soils and geomaterials, Casulli's scheme is promising for situations in which convergence is crucial. In the context of coupled hydromechanical flow-deformation analyses the advantages of constant, rather large time steps and the remarkable robustness offered by Casulli's scheme will certainly prove as the method of choice.

4 REFERENCES

Casulli, V., Zanolli, P.: A nested newton-type algorithm for finite volume methods solving Richards' equation in mixed form. SIAM Journal on Scientific Computing 32(4), 2255–2273 (2010). DOI10.1137/100786320. URL https://doi.org/10.1137/100786320

Celia, M.A., Bouloutas, E.T., Zarba, R.L.: A general mass-conservative numerical solution for the unsaturated flow equation. Water Resources Research 26(7), 1483–1496 (1990). DOI10.1029/WR026i007p01483

List, F., Radu, F.A.: A study on iterative methods for solving Richards' equation. Comput Geosci 20, 341–353 (2016). https://doi.org/10.1007/s10596-016-9566-3